

G. Brix
H. D. Nagel
G. Stamm
R. Veit
U. Lechel
J. Griebel
M. Galanski

Radiation exposure in multi-slice versus single-slice spiral CT: results of a nationwide survey

Received: 19 November 2002
Revised: 22 January 2003
Accepted: 4 February 2003
Published online: 10 April 2003
© Springer-Verlag 2003

G. Brix (✉) · R. Veit · U. Lechel · J. Griebel
Division of Medical Radiation Hygiene
and Dosimetry,
Institute of Radiation Hygiene,
Federal Office for Radiation Protection,
Neuherberg, Germany
e-mail: gbrix@bfs.de
Tel.: +49-1888-3332300
Fax: +49-1888-3332305

H. D. Nagel
Department of Science and Technology,
Philips Medical Systems,
Hamburg, Germany

H. D. Nagel
Manufacturers' Association
of Electromedical Equipment (ZVEI),
Frankfurt, Germany

G. Stamm · M. Galanski
Department of Radiology,
Hannover Medical School,
Hannover, Germany

M. Galanski
Quality Assurance Committee,
German Roentgen Society,
Germany

G. Brix
Institut für Strahlenhygiene,
Bundesamt für Strahlenschutz (BfS),
Ingolstädter Landstrasse 1,
85764 Oberschleissheim, Germany

Abstract Multi-slice (MS) technology increases the efficacy of CT procedures and offers new promising applications. The expanding use of MSCT, however, may result in an increase in both frequency of procedures and levels of patient exposure. It was, therefore, the aim of this study to gain an overview of MSCT examinations conducted in Germany in 2001. All MSCT facilities were requested to provide information about 14 standard examinations with respect to scan parameters and frequency. Based on this data, dosimetric quantities were estimated using an experimentally validated formalism. Results are compared with those of a previous survey for single-slice (SS) spiral CT scanners. According to the data provided for 39 dual- and 73 quad-slice systems, the average annual number of patients examined at MSCT is markedly higher than that examined at SSCT scanners (5500 vs 3500). The average effective dose to patients was changed from 7.4 mSv at single-slice to 5.5 mSv and 8.1 mSv at dual- and quad-slice scanners, respectively. There is a considerable potential for dose reduction at quad-slice systems

by an optimisation of scan protocols and better education of the personnel. To avoid an increase in the collective effective dose from CT procedures, a clear medical justification is required in each case.

Keywords Multi-slice spiral CT · Frequency of procedures · Radiation exposure · Nationwide survey · Recommendations for dose reduction

Introduction

Since its introduction by Hounsfield 30 years ago, computed tomography (CT) technology has made tremendous progress. After the introduction of single-slice

spiral CT (SSCT) into clinical practice in 1989 [1], the next considerable advance was the development of multi-slice spiral CT (MSCT) systems. The first step in this direction was taken in 1992 by Elscint with its “CT Twin” – a CT system with two contiguous detector

arcs [2]. Based on the experiences with this early dual-slice machine, several manufacturers in 1998 launched CT systems capable of scanning four slices simultaneously within a reduced scan time. The resulting increase in scanner performance can be used either to scan larger body regions in a reasonable time or to image a given body region in a shorter time or with an improved spatial resolution [3, 4, 5, 6, 7, 8]. These opportunities definitely increase the clinical efficacy of CT procedures and offer promising new applications in diagnostic imaging [3, 8, 9, 10], e.g. coronary angiography [11, 12, 13], coronary calcium scoring [14, 15], or virtual colonoscopy [16, 17]. On the other hand, however, the expanding use of MSCT systems in clinical practice may result in a considerable increase in both the frequency of CT procedures and patient exposure levels.

Data from various national surveys have confirmed, as a general pattern, the growing impact of CT as a major source of patient and population exposure [18]. In Germany, for example, it accounted for 4% of all X-ray examinations conducted in 1997, but for 37% of the resultant collective effective dose [19]. Therefore, many efforts have been undertaken by the European Union and its member states to limit radiation exposure arising from CT procedures as far as possible, e.g. by setting up guidelines on quality criteria for CT, including the specification of diagnostic reference levels [20]. In line with these efforts, the application of CT procedures without any clear medical justification or the application of non-optimised CT protocols must be avoided.

These basic principles have to be considered in particular during the current stage of introducing MSCT technology into clinical routine and, going along with that, the establishment of new examination protocols. Whereas there is an increasing number of investigations assessing the clinical potential of this innovative technology, patient exposure in MSCT as compared with SSCT has been evaluated in only a few studies [21, 22, 23] being neither representative for the various MSCT systems installed in hospitals and private practices nor for the large variety of imaging protocols used.

Therefore, it was the aim of this study (a) to gain an overview on the practice of MSCT examinations currently conducted in Germany, (b) to estimate mean values of scan parameters and dosimetric quantities for standard CT examinations, (c) to compare the estimated MSCT dose levels with those determined for SSCT systems in a previous nationwide survey [24], and (d) to propose modifications of the current practice, if necessary.

Materials and methods

Nationwide survey

In order to characterise MSCT practice in Germany, a survey was conducted from January to April 2002 in a concerted action by the German Roentgen Society (DRG), the Federal Office for Radiation Protection (BfS) and the Association of Manufacturers of Electromedical Equipment (ZVEI). To this end, all hospitals ($n=146$) and private practices ($n=61$) running an MSCT scanner at the beginning of 2002 were requested by letter to provide dose-relevant data on 14 standard CT examinations in a questionnaire.

Table 1 Definition of the 14 standard examinations and 4 additional examinations frequently carried out in a minor number of facilities. L_{st} standard scan length, $f_{mean,st}$ mean conversion coefficient for standard type of scanner (see text)

Examination	Abbreviation	Scan range		L_{st} (cm)	$f_{mean,st}$ (mSv/mGy·cm)	
		Upper limit	Lower limit		Male	Female
Brain	BR	Vertex	Base of skull	12	0.0022	0.0024
Face and sinuses	FS	Frontal sinus	Shenoidal sinus	11	0.0022	0.0024
Face and neck	FA/NE	Sella	Inferior extremity of thyroid gland	18	0.0029	0.0035
Chest	CH	C7/T1	Sinus	27	0.0068	0.0088
Abdomen and pelvis	AB/PE	Subphrenic space	Symphysis	42	0.0072	0.0104
Pelvis	PE	Inferior extremity of kidney	Symphysis	24	0.0062	0.0112
Liver/kidney	LI/KI	Subphrenic space	Inferior extremity of kidney	18	0.0085	0.0096
Whole trunk	WT	C7/T1	Symphysis	66	0.0070	0.0098
Aorta, thoracic	AT	Clavicle	Subphrenic space	26	0.0071	0.0092
Aorta, abdominal	AA	Subphrenic space	Hip	28	0.0070	0.0110
Pulmonary vessels	PV	Clavicle	Subphrenic space	16	0.0073	0.0096
Pelvis, skeleton	PS	Iliac crest	Ischial bone	22	0.0065	0.0116
Cervical spine	CS	C1	C7	10	0.0049	0.0053
Lumbar spine	LS	L1	S1	15	0.0081	0.0094
Extremities	EX					
Coronary CTA	COAN	T7/T8	Sinus	12	0.0071	0.0105
Calcium scoring	CASO	T7/T8	Sinus	12	0.0071	0.0105
Virtual colonoscopy	VICO	Subphrenic space	Symphysis	42	0.0072	0.0104

A description of the standard examinations, which are defined in exactly the same way as in the previous reference survey concerning SSCT examinations [24], is given in Table 1. Facilities that did not respond to our inquiry were contacted a second time in order to increase the response rate as far as possible.

Besides the type and year of installation of their MSCT system, holders were requested to provide for each of the 14 predefined standard examinations and, if applicable, for further special procedures frequently performed at their scanner the number of procedures per year and the relevant scan parameters (tube potential, electrical current, rotation time, slice collimation, pitch, scan length, thickness of reconstructed images, and number of series) in the questionnaire. For the purpose of further evaluation, data were transferred to a worksheet file (Excel 7.0, Microsoft, Seattle, Wash.).

Dosimetry

For the various CT examinations and scanners considered, patient exposure was estimated using the complex dosimetric formalism implemented in the program CT-EXPO (version V1.1, Hamburg/Hannover, Germany), which has been described elsewhere in detail [25, 26]. In brief, calculation of the effective dose E_{ser} (in mSv) for a single CT scan series is based on the following equation:

$$E_{ser} = CTDI_{air} \cdot \frac{1}{p} \cdot \sum_{z_L}^{z_U} f(z) \quad (1)$$

with $CTDI_{air}$ the well-known CT dose index free-in-air (in mGy), i.e. the dose on the axis of rotation of the scanner, and $f(z)$ the scanner-specific conversion factor between $CTDI_{air}$ and E_{ser} for a single slice placed at the axial position z within the scan region $z_L \leq z \leq z_U$ in an anthropomorphic phantom mimicking either an adult male or female patient; p is the pitch factor defined as the ratio of table movement per gantry rotation and beam collimation $N \cdot h_{col}$ with N the number of slices acquired simultaneously and h_{col} the nominal slice (or detector) collimation during data acquisition (see Fig. 1). For the calculation of the effective dose, tissue weighting factors developed by the ICRP from a reference population of equal numbers of both genders and a wide range of ages were used [27]. In the definition of the effective dose they apply to either gender.

In practice, a convenient assessment of $CTDI$ can be made using a pencil ionisation chamber with an active length of 100 mm. This measurement is carried out either free-in-air ($CTDI_{air}$) or, as is usually done, at the centre ($CTDI_{100,c}$) and at the periphery ($CTDI_{100,p}$) of the standard head or body CT dosimetry phantom. On the assumption that the dose decreases linearly with the radial position from the surface to the centre of the phantom, the average dose can be characterised by the weighted $CTDI$ as follows:

$$CTDI_w = \frac{1}{3}CTDI_{100,c} + \frac{2}{3}CTDI_{100,p} \quad (2)$$

In contrast to this quantity, the normalised weighted $CTDI$

$${}_nCTDI_w = \frac{1}{Q_{el}} \cdot CTDI_w, \quad (3)$$

with Q_{el} the radiographic exposure (in mAs), is a scanner-specific quantity which comprises all output characteristics of a given type of scanner and thus can be used for further dose assessment [20]. The relation between $CTDI_w$ and $CTDI_{air}$ depends on the scanner type used for the examination and on the dosimetric phantom considered. For the purpose of dose estimation, the ratio of both quantities is determined for the standard head (H) and body (B) CT dosimetry phantom

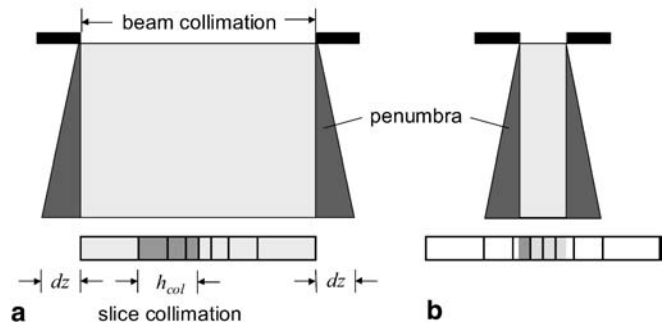


Fig. 1a, b Design of a quad-slice CT scanner with a non-isotropic adaptive detector array. By changing beam collimation and electronically binning of different numbers of adjacent detector elements together, images from four slices with variable thickness can be acquired simultaneously. **a** Four thick slices and **b** four thin slices. The figure reveals that the relative contribution of overbeaming (dark grey penumbra) to total patient exposure becomes more relevant with decreasing slice thickness. The overbeaming parameter dz represents the width of the penumbra at both sides of the detector array

$$P_H = \frac{CTDI_{w,H}}{CTDI_{air}} \quad \text{and} \quad P_B = \frac{CTDI_{w,B}}{CTDI_{air}}, \quad (4)$$

respectively. Finally, two further operational quantities are defined: the effective weighted $CTDI_{w,eff} = CTDI_w/p$ and the dose-length product per scan series $DLP_{ser} = CTDI_{w,eff} L$ characterising the integral dose for a complete CT scan series over an axial length L .

With these definitions, Eqs. (1) can be rewritten as

$$E_{ser} = \frac{{}_nCTDI_{w,H/B}}{P_{H/B}} \cdot Q_{el} \cdot \frac{1}{p} \cdot L \cdot f_{mean} \quad (5)$$

with $f_{mean} = \sum f(z)/L$ the scanner-specific average conversion factor over the scan length $L = z_U - z_L$.

Unfortunately, scanner-specific conversion factors are not available for most of the CT scanners and the vast variety of scan parameters applied in clinical routine; therefore, conversion factors determined for a standard CT scanner ($f_{mean,st}$) are used and corrected properly. The standard conversion factors $f_{mean,st}$ are calculated from organ-specific conversion factors derived by Zankl et al. [28] for the anthropomorphic mathematical phantoms ADAM and EVA [29] by means of Monte-Carlo calculations for the CT scanner SOMATOM DRH (Siemens) working without beam shaping filter at a voltage of $U=125$ kV and a filtration of 2 mm aluminium and 0.2 mm copper. Corrections are performed according to

$$f_{mean} = f_{mean,st} \cdot k_{CT} \quad (6)$$

where k_{CT} is a correction factor taking into account differences in scanner geometry and the effect of beam shaping filters. Correction factors k_{CT} are determined following the concept presented by Shrimpton et al. [30].

Moreover, since for many scanners ${}_nCTDI_{w,H/B}$ is not known for all voltages and slice collimations applied in clinical routine, this quantity is calculated from a reference value ${}_nCTDI_{w,H/B,ref}$ determined for a voltage U_{ref} and a slice collimation h_{ref} applying appropriate correction factors:

$${}_nCTDI_{w,H/B} = {}_nCTDI_{w,H/B,ref} \cdot k_{OB} \cdot \left(\frac{U}{U_{ref}} \right)^{2.5} \quad (7)$$

Table 2 Summary of multi-slice spiral CT scanners for which information was provided by the owners along with characteristic scanner parameters used for the estimation of dosimetric quantities. *Number* no. of simultaneously acquired slices, U_{ref} reference voltage for ${}^nCTDI_{w,H/B}$, h_{ref} slice collimation for ${}^nCTDI_{w,H/B}$, d_z width of penumbra, ${}^nCTDI_{w,H/B}$ normalised $CTDI_w$ for head or body mode, P_{BH} phantom factor for head or body mode, k_{CT} scanner specific correction factor

Manufacturer	Scanner	No. of questionnaires filled out	Number	U_{ref} (kV)	h_{ref} (mm)	d_z (mm)	Head mode			Body mode		
							${}^nCTDI_{w,H}$ (mGy/mAs)	P_H	k_{CT}	${}^nCTDI_{w,B}$ (mGy/mAs)	P_B	k_{CT}
General Electric	HiSpeed NX/i	4	2	120	10	0	0.147	0.64	0.80	0.066	0.29	0.65
General Electric	Lightspeed QX/i	10	4	120	5	3.0/4.0 ^a	0.182	0.64	0.80	0.094	0.39	0.80
General Electric	Lightspeed Plus	5	4	120	5	3.0/4.0 ^a	0.182	0.64	0.80	0.94	0.39	0.80
General Electric	Lightspeed Ultra	1	8	120	2.5	3.0/4.0 ^a	0.182	0.64	0.80	0.094	0.39	0.80
Elscent/ Marconi/Philips	CT-Twin, Mx Twin, Twin II	30	2	120	10	0.8	0.105	0.59	0.70	0.043	0.24	0.50
Marconi/Philips	Mx8000 Dual	2	2	120	5	0.6	0.149	0.73	0.90	0.073	0.36	0.80
Marconi/Philips	Mx8000 Quad	7	4	120	5	1.7	0.130	0.75	0.90	0.067	0.39	0.80
Siemens	Volume Zoom	41	4	120	5	1.7	0.200	0.76	0.90	0.083	0.49	1.00
Siemens	Volume Access	2	2	120	10	0.8	0.200	0.76	0.90	0.083	0.49	1.00
Toshiba	Asteion Dual	1	2	120	10	3.3	0.298	0.65	0.80	0.149	0.32	0.65
Toshiba	Asteion Multi	1	4	120	5	3.8	0.283	0.65	0.80	0.141	0.32	0.65
Toshiba	Aquilion	9	4	120	5	3.0	0.188	0.69	0.80	0.105	0.31	0.65

^a Value depends on focal spot size

The factor k_{OB} , correcting for differences in slice collimation and for overbeaming effects, is determined analytically using the scanner specifications given in Table 2 according to:

$$k_{OB} = \frac{h_{ref} \cdot (N \cdot h_{col} + dz)}{h_{col} \cdot (N \cdot h_{ref} + dz)}, \quad (8)$$

where dz , the overbeaming parameter, is equal to the width (in z direction) of the rectangle which is obtained by combining the penumbra triangles at both edges of the dose profile at the detector array (see Fig. 1).

With these approximations, the effective dose was calculated according to Eqs. (5), (6), (7) and (8) for the 14 standard examinations on the basis of (a) the scan parameters h_{col} , p , L , Q_{el} , and U provided by the users in the questionnaire, and (b) representative values stored in a look-up table for $P_{H/B}$, $nCTD_{w,H/B,ref}$, k_{OB} , k_{CT} and $f_{mean,st}$ characterising the type of scanner and the body region considered. Scanner parameters are summarised in Table 2 for the relevant MSCT systems. Effective doses were calculated first separately for the adult mathematical phantoms ADAM and EVA with gender-specific characteristics and were then averaged.

To experimentally validate the complex theoretical formalism applied for the estimation of the effective dose in the present and the previous reference survey, measurements were performed with an anthropomorphic whole-body Alderson RANDO phantom (Alderson Research Laboratories, Long Island City, N.Y.) transsected horizontally into 2.5-cm-thick slices with holes drilled on a 3×3-cm grid. The holes were plugged either by tissue-equivalent pins or by holder pins for LiF thermoluminescent dosimeters (TLD-100; Bricron-Harshaw, Cleveland, Ohio). The TLDs were calibrated using conventional X-ray equipment with a tube potential of 120 kV and a filter of 5 mm aluminium to approximate the radiation quality of CT scanners. Calibration, annealing and readout of the TLDs was performed following a standard procedure [31].

Measurements were performed at four SSCT (GE LX/i, Philips Tomoscan AV, Siemens Somatom Plus 4, Toshiba XVision) and four MSCT systems (GE Lightspeed QX/i, Philips Mx8000 Quad, Siemens Volume Zoom, Toshiba Aquilion). At each scanner, three body regions of the Alderson phantom (head, chest and pelvis) were imaged using protocols frequently carried out at the selected MSCT and SSCT scanners for the standard examinations (BR, CH and PE; Table 1). The TLDs were suitably distributed throughout the Alderson phantom to sample the non-uniform dose distribution associated with the CT procedures. Based on the evaluated dose values, organ doses and the effective dose were estimated following a scheme similar to that presented by Huda and Sandison [32].

Presentation and statistical analysis of data

Mean values of the most important scan parameters and dosimetric quantities determined for dual- and quad-slice CT scanners were analysed for the 14 standard examinations relative to the corresponding mean values which was established in the previous nationwide survey for 398 CT scanners installed between January 1996 and June 1999. This group of newer CT scanners, which forms a subgroup of the CT systems considered in the previous reference survey, consists of more than 98% of SSCT scanners.

Statistical evaluations were performed with the statistical program package SigmaStat (version 2.03; SPSS Science Software, Erkrath, Germany) at a significance level of $p=0.05$. For the scan parameters and dosimetric quantities considered, differences in the median values determined for single-, dual- and quad-slice CT scanners were evaluated pairwise for each of the 14 standard CT examinations using the non-parametric Dunn's test for multiple comparisons. Correlation between calculated and measured effective doses was evaluated by calculating Spearman's rank correlation coefficient r_s . In addition, a linear regression analysis between the two dose quantities was performed.

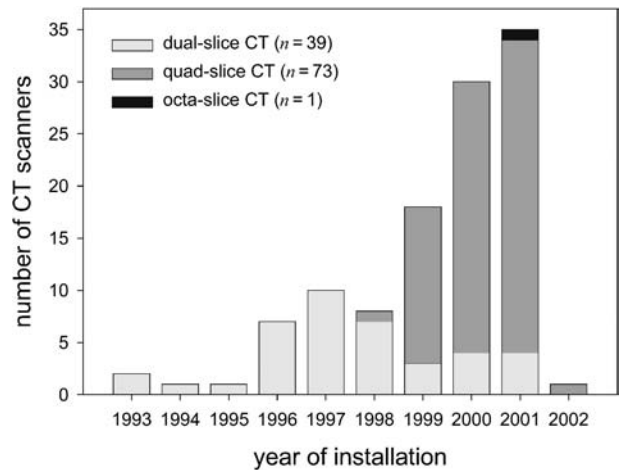


Fig. 2 Year of installation of the 113 MSCT scanners for which information was provided in the questionnaires

Results

Of the 207 owners of MSCT scanners in Germany, 113 responded to our inquiry and filled out the questionnaire. This corresponds to an overall response rate of 55% (60% for hospitals and 43% for private practices). More than 70% of all questionnaires, however, were filled out incompletely or showed obvious mistakes. In these cases, users were contacted in order to get correct data.

With respect to the scanner type, the response rate was 49% (39 of 79) for dual-slice and 58% (74 of 128) for quad- and octa-slice CT scanners; details are given in Table 2. Due to historical and national reasons, the majority of dual-slice and quad-slice scanners were of the type "CT Twin" (30 of 39) and "Volume Zoom" (41 of 73), respectively. According to the information provided in the questionnaires, 87% of the MSCT scanners that have been installed since 1999 are quad- or octa-slice systems (Fig. 2).

As shown in Fig. 3, the annual number of examinations carried out per MSCT scanner varied considerably between the facilities which responded to our inquiry. Whereas at approximately 11% of the scanners between 10,000 and 15,000 procedures were performed per year, the mean annual number of procedures was approximately 5500 (dual-slice scanner: 4900; quad-slice scanner: 5700). In comparison with the average number of 3500 procedures conducted at SSCT systems, the rise at quad-slice systems is statistically highly significant ($p<0.001$). In addition to the standard examinations defined in Table 1, four additional procedures were frequently conducted in a minor number of facilities: examinations of the skeleton of upper and lower extremities, coronary angiography, coronary calcium scoring, and virtual colonoscopy. The percent contribution of the different CT examinations to the total number of proce-

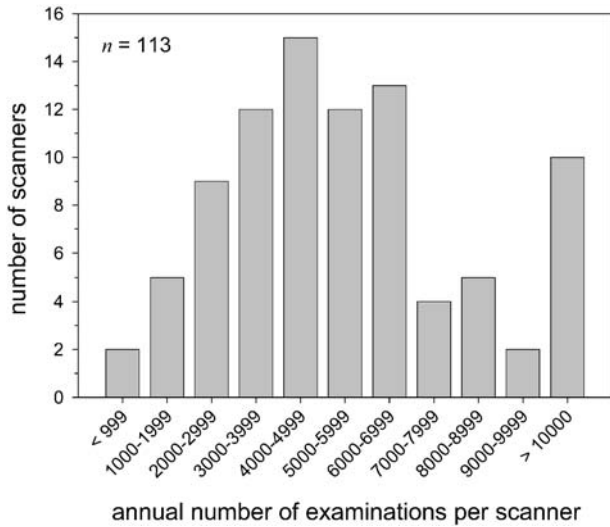
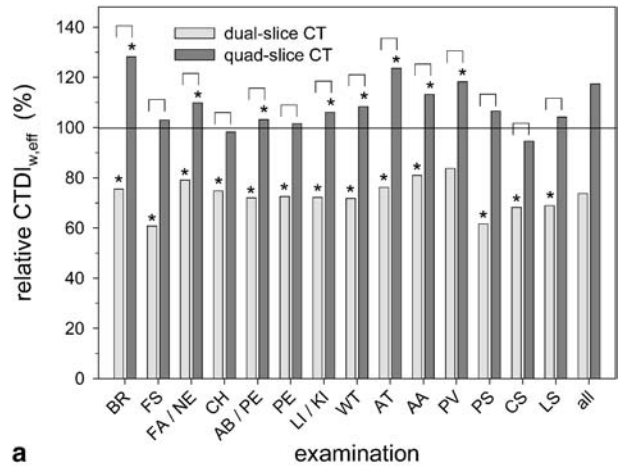


Fig. 3 Distribution of the number of MSCT examinations per year and scanner. Data are based on information provided for 113 MSCT scanners

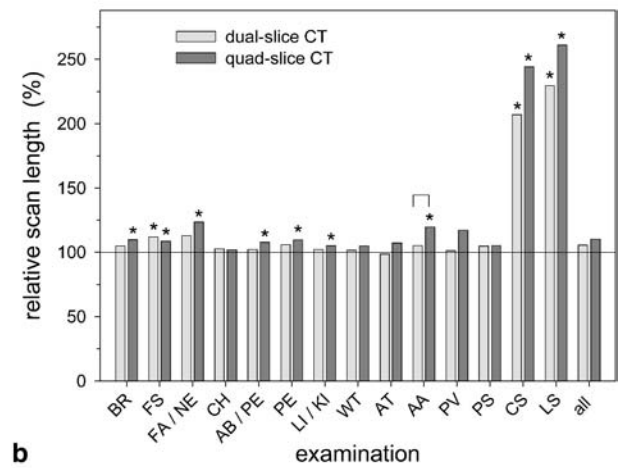
dures reported, as well as the corresponding mean scan parameters and dosimetric quantities, are summarised in Table 3. For comparison, the values obtained for SSCT systems in the previous survey are given in Table 4. For a more detailed analysis, mean values of the most relevant scan parameters and dosimetric quantities determined for dual- and quad-slice CT scanners are plotted in Figs. 4, 5, 6 and 7 for the 14 standard examinations relative to the corresponding mean values established for SSCT scanners.

Figure 4a reveals that the mean $CTDI_{w,eff}$ determined for quad-slice scanners is higher for all standard examinations compared with dual-slice and for most examinations also compared with single-slice CT systems. Taking into account the different frequencies of the 14 standard examinations, the average $CTDI_{w,eff}$ over all examinations is increased for quad-slice scanners, in comparison with single- and dual-slice systems, by 17 and 59%, respectively. The second major parameter determining radiation exposure of patients undergoing a CT procedure is the scan length L . Figure 4b demonstrates that the scan length is only slightly increased in MSCT compared with SSCT for 12 of the 14 standard examinations, whereas a large and highly significant increase by up to 160% is observed for examinations of the cervical and lumbar spine. Results of the DLP per scan series – which is defined as the product of both quantities, $DLP_{ser} = CTDI_{w,eff} \cdot L$ – are presented in Fig. 4c. In comparison with SSCT examinations, this quantity is significantly higher for 13 of the 14 standard examinations carried out at quad-slice scanners by up to 150% (on average by 29%). On the other hand, a decrease by 22% is observed for the average DLP_{ser} determined for dual-slice scanners.

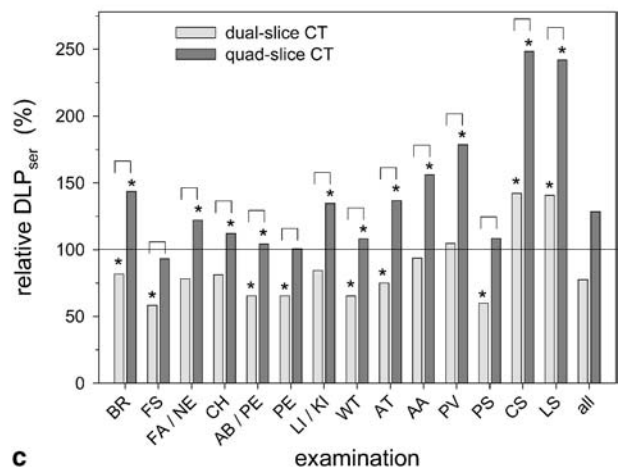
In order to characterise CT procedures completely, the number of series, N_{ser} , i.e. the number of CT scans



a



b



c

Fig. 4 Mean values of **a** $CTDI_{w,eff}$, **b** scan length L and **c** DLP per scan series determined at dual- and quad-slice scanners for the 14 standard CT examinations defined in Table 1 and the corresponding mean values averaged by weight over all CT examinations. Data are presented relative to the corresponding mean values determined in a previous survey [24], for SSCT scanners installed between January 1996 and June 1999 (see Table 4). Significant differences ($p < 0.05$) in the median values between the three scanner groups are marked by *asterisk* (dual vs single and quad vs single) or by *square bracket* (\square) (dual vs quad)

Table 3 Summary of measurement parameters used at multi-slice spiral CT (p pitch, h_{rec} thickness of reconstructed images, L scan length, N_{ser} no. of scan series, (MSCT) scanners in Germany in 2002. Given are mean values of scan parameters $CTDI_{weff}$ -weighted effective CTDI, $CTDI_w$ -weighted CTDI, DLP dose-length product, and dose quantities evaluated from data provided for 113 MSCT scanner in questionnaires. U tube voltage, Q_{el} electrical current-time product, h_{col} slice collimation, E_{ser} effective dose

Examination ^a	Scan parameters										Dose quantities					
	Relative frequency (%)	No. of facilities providing data	U (kV)	Q_{el} (mAs)	h_{col} (mm)	p	h_{rec} (mm)	L (cm)	N_{ser}	Per slice or rotation		Per scan series		Per examination		
										$CTDI_{weff}$ (mGy)	$CTDI_w$ (mGy)	DLP_{ser} (mGy·cm)	E_{ser} (mSv)	DLP_{exam} (mGy·cm)	E_{exam} (mSv)	
BR	27.1	104	122	317	5.7	1.0	7.3	13.2	1.3	60.6	58.4	813	2.2	1016	2.8	
FS	4.4	102	123	123	1.7	1.1	2.4	10.2	1.0	26.7	28.2	272	0.8	283	0.8	
FA/NE ^b	3.6	99	122	202	3.0	1.1	4.2	19.5	1.1	14.4	17.2	288	1.9	302	2.0	
CH	15.7	108	128	163	4.0	1.4	6.3	31.0	1.0	10.9	14.8	339	5.5	350	5.7	
AB/PE	17.6	106	121	200	4.3	1.3	6.6	41.9	1.5	12.6	15.6	529	9.7	790	14.4	
PE	2.6	94	123	203	4.0	1.2	6.0	23.6	1.2	14.8	17.1	349	6.3	398	7.2	
L/KI	5.9	103	121	191	3.8	1.2	5.8	22.7	2.1	12.8	15.5	292	5.5	612	11.5	
WT	4.1	76	124	194	4.0	1.3	6.6	65.4	1.2	12.8	16.7	836	14.5	1027	17.8	
AT	1.4	90	123	176	2.7	1.4	4.1	28.5	1.1	12.6	16.3	361	6.1	398	6.7	
AA	1.8	91	122	197	2.8	1.4	4.2	37.5	1.2	12.8	17.3	484	9.0	552	10.3	
PV	1.8	91	124	179	1.9	1.4	3.2	23.5	1.0	12.8	17.7	300	5.2	310	5.4	
PS	1.5	88	129	204	2.3	1.2	3.4	22.3	1.0	19.4	21.8	438	8.2	440	8.2	
CS ^b	3.2	103	128	243	1.7	1.0	2.1	10.0	1.0	27.0	26.0	275	2.9	277	2.9	
LS	5.9	107	130	285	2.3	1.0	2.8	13.5	1.0	32.4	30.3	441	8.1	445	8.1	
EX	1.8	68	122	120	1.1	1.1	1.7	12.6	1.0	14.4	14.8	169	-	171	-	
COAN	1.6	21	121	133	1.2	0.4	1.7	13.1	1.1	43.1	15.1	564	10.2	583	10.5	
CASO	1.5	121	88	2.4	0.7	2.7	13.8	1.0	12.4	8.7	171	3.1	171	3.1		
VICO	10	120	138	1.2	1.5	2.5	37.7	1.2	11.4	16.1	440	8.0	567	10.2		

^a Abbreviations are defined in Table 1

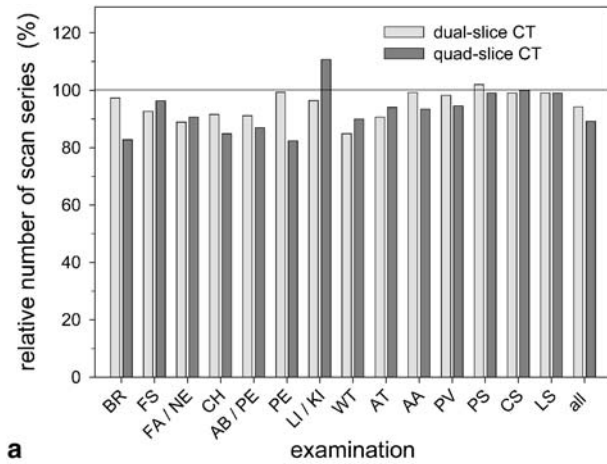
^b Body mode

Table 4 Summary of measurement parameters used at single-slice spiral CT (SSCT) scanners in Germany in the year 1999. Given are mean values for scan parameters and dose quantities evaluated in a previous nationwide survey for 398 SSCT scanners that were installed between January 1996 and June 1999. U tube voltage, Q_{el} electrical current-time product, h_{col} slice collimation, p pitch, L scan length, N_{ser} no. of scan series, $CTDI_{w,eff}$ weighted effective CTDI, $CTDI_w$ weighted CTDI, DLP dose-length product, E effective dose. [From 24]

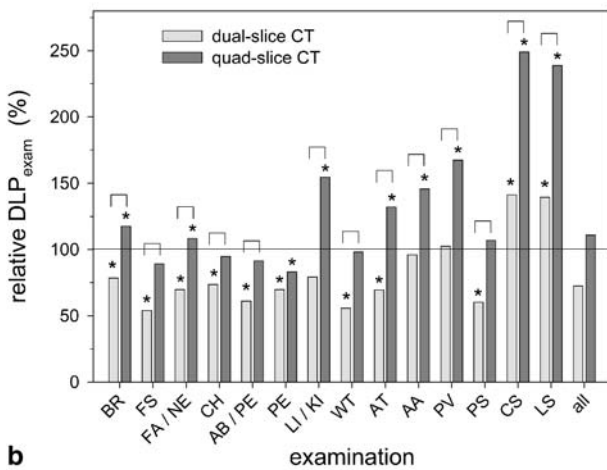
Examination	Scan parameters					Dose quantities								
	Abbreviation ^a	No. of facilities providing data	U (kV)	Q_{el} (mAs)	h_{col} (mm)	p	L (cm)	N_{ser}	Per slice or rotation		Per scan series		Per examination	
									$CTDI_{w,eff}$ (mGy)	$CTDI_w$ (mGy)	DLP_{ser} (mGy·cm)	E_{ser} (mSv)	DLP_{exam} (mGy·cm)	E_{exam} (mSv)
BR	387		129	296	8.2	1.0	12.3	1.5	56.1	56.7	673	1.9	980	2.8
FS	379		127	188	3.1	1.3	9.3	1.1	30.6	35.3	336	1.0	369	1.1
FA/NE ^b	365		126	185	4.6	1.3	16.2	1.2	14.5	18.2	261	1.7	308	2.0
CH	385		127	165	7.9	1.4	30.3	1.2	12.3	16.6	331	5.2	398	6.2
AB/PE	377		123	198	8.6	1.4	39.6	1.7	13.9	18.5	585	10.3	981	17.2
PE	367		127	213	7.8	1.4	21.8	1.3	16.6	21.4	398	6.9	511	8.8
LI/KI	375		123	201	7.1	1.4	21.8	1.9	13.9	18.8	250	4.6	480	8.7
WT	139		124	192	8.5	1.4	62.9	1.4	13.4	17.7	882	14.9	1214	20.5
AT	193		125	176	6.1	1.5	27.2	1.2	11.7	16.9	305	5.0	352	5.8
AA	203		123	193	6.2	1.5	32.5	1.2	12.5	17.8	350	6.3	420	7.6
PV	180		127	176	4.8	1.5	21.0	1.1	12.0	17.3	192	3.3	209	3.6
PS	328		130	244	4.6	1.3	21.2	1.0	21.8	26.0	480	8.6	487	8.8
CS ^b	331		131	315	2.8	1.1	4.3	1.0	31.9	33.9	128	2.1	129	2.1
LS	384		132	337	3.2	1.1	5.4	1.0	35.7	37.1	214	2.7	216	2.7

^a Abbreviations are defined in Table 1

^b Body mode



a

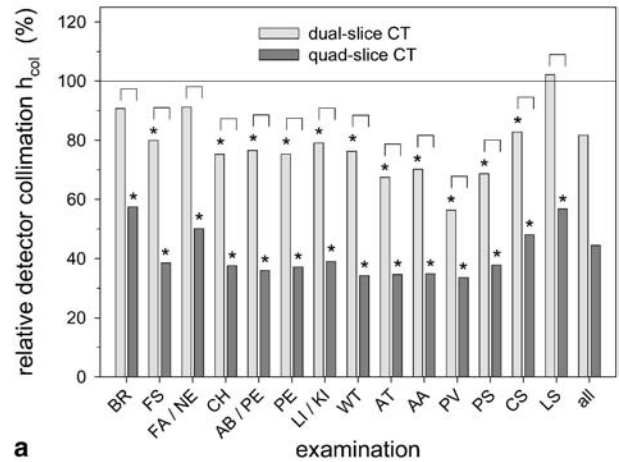


b

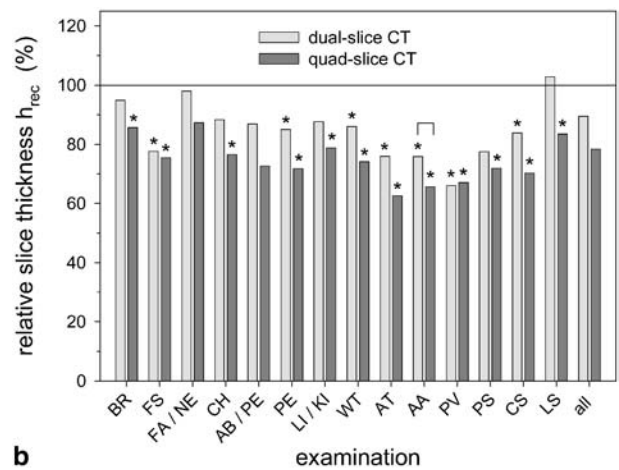
Fig. 5 Mean values of **a** the number N_{ser} of scan series and **b** the DLP_{exam} per examination determined at dual- and quad-slice scanners for the 14 standard CT examinations defined in Table 1 and the corresponding mean value averaged by weight over all CT examinations. For details see Fig. 4

performed before and after administration of a contrast agent, must be taken into account. As shown in Fig. 5a, this quantity has been reduced – with the exception of liver examinations at quad-slice systems – for all standard examinations conducted at MSCT scanners (on average by 6 and 11% for dual-slice and quad-slice systems, respectively). The DLP per examination, $DLP_{exam} = DLP_{ser} N_{ser}$, is plotted in Fig. 5b for the 14 standard examinations carried out at MSCT scanners relative to the corresponding mean values evaluated for SSCT systems. Compared with SSCT scanners, DLP_{exam} is increased on average by 11% for quad-slice scanners, whereas it is reduced by 28% for dual-slice scanners.

An essential difference in CT practice between dual- and quad-slice scanners is the significantly reduced slice collimation for CT examinations performed at quad-slice



a



b

Fig. 6 Mean values of **a** detector collimation h_{col} and **b** reconstructed slice thickness h_{rec} determined at dual- and quad-slice scanners for the 14 standard CT examinations defined in Table 1 and the corresponding mean values averaged by weight over all CT examinations. For details see Fig. 4

scanners as shown in Fig. 6a (average: $h_{col}^{single} = 7.1$ mm, $h_{col}^{dual} = 5.8$ mm, $h_{col}^{quad} = 3.2$ mm).

On the other hand, Fig. 6b reveals that the thickness of reconstructed slices is more similar for all types of scanners (average: $h_{rec}^{single} = 7.1$ mm, $h_{rec}^{dual} = 6.4$ mm, $h_{rec}^{quad} = 5.6$ mm).

Nevertheless, reconstructed slice thickness is significantly reduced when MSCT systems are used.

The relevant quantity for risk assessment is the effective dose per examination, which depends not only on the scan parameters chosen and the number of CT scan series performed, but also on the body region examined. The effective dose per examination is plotted in Fig. 7 for the 14 standard procedures considered. Averaged over all examinations it is increased by 10% and decreased by 26% for quad-slice and for dual-slice scan-

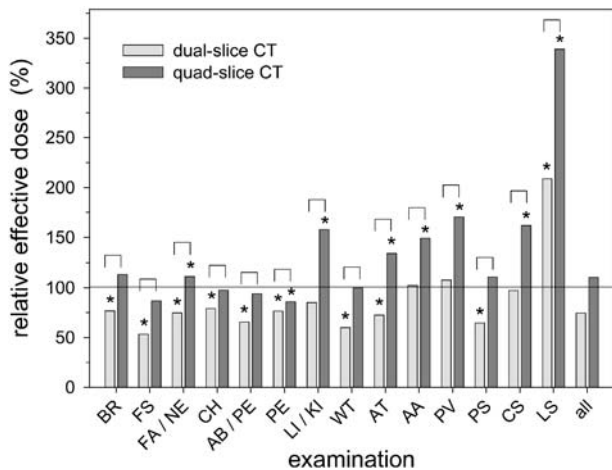


Fig. 7 Mean effective dose E_{exam} determined at dual- and quad-slice scanners for the 14 standard CT examinations defined in Table 1 and the corresponding mean value averaged by weight over all CT examinations. For details see Fig. 4

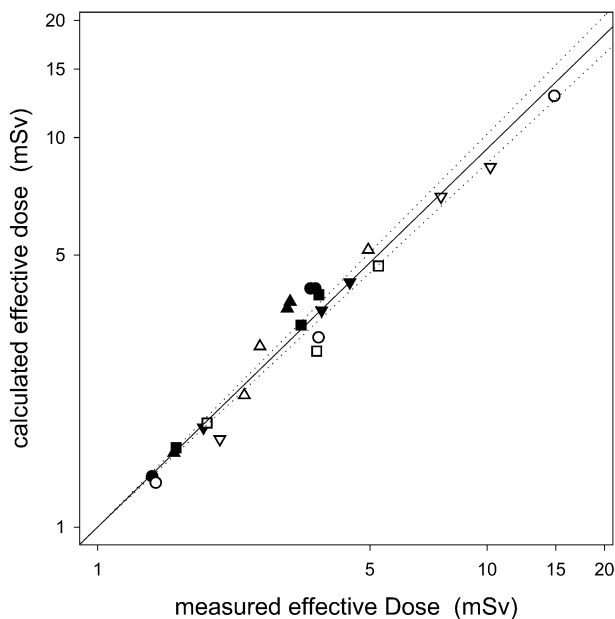


Fig. 8 Statistical relation between calculated and measured effective dose values determined for three representative CT examinations (head, chest and pelvis) carried out at four SSCT (filled symbols) and four (open symbols) MSCT systems of different manufactures each (GE, Philips, Siemens, Toshiba). Spearman's rank correlation test yielded a significant correlation between the parameters ($p < 0.001$, $r_s = 0.929$). The solid line gives the result of a linear regression analysis through origin and the dotted curves the 95% confidence interval

ners compared with the same investigations carried out at SSCT machines, respectively.

Effective doses calculated for representative CT examinations of the head, chest and pelvis for eight differ-

ent types of SSCT and MSCT scanners are plotted in Fig. 8 vs the corresponding dose values determined experimentally on the basis of TLD measurements at the Alderson phantom. According to Spearman's rank test there is a highly significant correlation ($p < 0.001$, $r_s = 0.929$) between calculated and measured data. Linear regression analysis yielded a slope of 0.91 for the regression line through the origin.

Discussion

This article provides, for the first time, a comprehensive overview of the practice of MSCT examinations carried out in both hospitals and private practices in Germany. The results presented were derived from indications in the questionnaires filled out by 55% of all facilities who were running at least one MSCT system at the beginning of 2002; therefore, they have a high level of reliability from a statistical point of view. For benchmarking, data determined in this study for 14 standard CT examinations were compared with results obtained in a previous nationwide survey for the same examinations at newer SSCT systems which were installed between January 1996 and June 1999.

As an overall trend, our survey reveals that radiation exposure of patients – as described by the dosimetric quantities DLP_{exam} and E_{exam} – is increased for CT procedures performed at quad-slice compared with single-slice CT systems, whereas it is reduced for dual-slice systems. There are three general reasons for this trend, which are more related with technical features of quad-slice systems and general concepts of CT scanning at these systems than with the specific type of examination: firstly, at MSCT scanners with more than two detector rows, each detector contributes to every reconstructed image, and therefore the image noise and the slice sensitivity profile for each slice need to be similar to reduce image artefacts. To accommodate this condition, beam collimation is usually adjusted in such a way that the focal spot-collimator blade penumbra falls outside the edge detectors (see Fig. 1). The resulting overbeaming causes an increase of radiation dose compared with single- and (most) dual-slice scanners, where the collimator width is always smaller than the maximum detector width [33]. As shown in Fig. 1, this effect becomes more relevant for thinner slices, which are preferred at quad-slice in contrast to single- and dual-slice systems (see Fig. 6a); however, with the availability of MSCT systems capable of scanning more than four slices simultaneously ($n=8, 16, \dots$) overbeaming will become less significant in the future.

Secondly, utilising the improved tube output at quad-slice scanners, narrow slice collimation is frequently used for CT examinations at these machines since it offers the possibility to retrospectively reconstruct CT im-

ages or maximum intensity projections (MIPs) in all directions with an almost identical in-plane resolution. Although isotropic voxel imaging is a sound approach, it runs the risk of selecting radiographic exposure values (in milliamperes) with respect to the narrow slice collimation, in order to compensate for the increased noise, and not to the thickness of the reconstructed CT images. Both parameters differ considerably at quad-slice scanners as demonstrated by Fig. 6a and b, respectively. Moreover, it is noted that detail contrast is greatly enhanced with narrow slice collimation due to the reduction of partial-volume effects and thus contrast-to-noise ratio (CNR) is significantly improved even in the presence of increased noise. This fundamental advantage of MSCT, which makes increased milliamperage settings obsolete, has not sufficiently been appreciated by the majority of users up to now.

Thirdly, at the majority of quad-slice scanners used in Germany, radiographic exposure Q_{el} is automatically adapted in such a way that the effective radiographic exposure per slice Q_{el}/p is held constant when the pitch is changed. As a consequence, the dose per slice (i.e. $CTDI_{w,eff}$) is no longer influenced by the pitch selected as in SSCT. Since this concept is rarely understood by users, especially by those with a strong background in SSCT, they frequently underestimate patient exposure when choosing a pitch of $p > 1$.

Figure 5b reveals that the DLP per examination – and in almost the same manner the effective dose per examination (Fig. 7) – is markedly increased in comparison with SSCT for various CT procedures performed at quad-slice and, in contrast to the overall trend but to a smaller extent, also at dual-slice systems. This concerns especially investigations (a) of the liver which are frequently carried out at quad-slice systems as multiphase scans (see Fig. 5a) to improve detection and characterisation of liver lesions by a separation of distinct circulatory phases [34], (b) of the aorta and pulmonary vessels which are conducted with narrow slice collimation and increased DLP_{scan} with regard to the generation of high-quality MIPs, and (c) of the cervical and lumbar spine which are no longer scanned over the relevant segments only but rather over the complete section of the spine. Taking the different frequencies of the 14 standard applications into account, the mean DLP per examination evaluated in this study has been changed from 683 mGy·cm at SSCT scanners to 495 and 757 mGy·cm at dual-slice and quad-slice systems, respectively; thus, this dosimetric quantity is increased at quad-slice scanners by 53% on average with respect to the same procedures carried out on dual-slice systems.

There is another noteworthy observation concerning examinations of the whole trunk, which are usually carried out for tumour staging and in the case of multiple trauma patients. In the majority of CT facilities, the relative frequency of this type of examination is correspond-

ingly low (<5%). According to the frequency data indicated in the questionnaires for quad-slice systems, however, CT scanning of the whole trunk is performed in some facilities in up to 40% of all CT examinations. Since this procedure results in a rather high level of patient exposure (Table 3), it has to be limited to the above-mentioned cases with a clear medical justification. The CT examinations of the whole trunk or even of the whole body must not be established as a new standard in clinical CT practice.

The major challenge in performing a nationwide survey aimed at assessing radiation exposure of patients undergoing CT procedures is to estimate the effective dose for the vast variety of imaging protocols and CT scanners which are used both in hospitals and private practices. In the present and previous reference study, a complex dosimetric formalism was applied to calculate approximately the effective dose on the basis of scan parameters, provided by the users in a questionnaire, together with representative parameters characterising the type of CT scanner used and the body region irradiated. To evaluate the reliability of this approach, measurements were performed with an anthropomorphic whole-body phantom at four SSCT and four MSCT scanners of different manufactures each. Statistical evaluation yielded a high linear correlation between measured and calculated dose values, although larger differences of up to 29% were observed for a few examinations. These differences are mainly due to two factors: firstly, the mathematical phantoms ADAM and EVA have not the same size and configuration as the anthropomorphic Alderson phantom. As a consequence, tissues and organs with higher or lower tissue weighting factors may be partly in the scan region in one phantom but not in the other. Secondly, a mean $nCTDI_{w,H/B}$ value is used for each type of scanner (Table 2), which may differ from the actual value at the specific scanner considered. It is mentioned, however, that both effects cancel out by determining the effective dose for larger groups of patients and scanners as in the present study. Taking these considerations into account, the data presented in Fig. 8 validates the accuracy of the effective doses summarised in Tables 3 and 4 for standard examinations performed at MSCT and SSCT scanners, respectively. It is noted, moreover, that effective doses summarised in Table 3 and 4 are average values ignoring gender specific differences. Actually, the effective dose for all 14 standard CT examinations considered is somewhat higher for females than for males.

As a major result, our investigation reveals that the mean effective dose to patients has been changed from 7.4 mSv at SSCT scanners to 5.5 and 8.1 mSv at dual-slice and quad-slice systems, respectively; thus, the effective dose at quad-slice scanners is increased by approximately 47% on average with respect to the same procedures carried out at dual-slice systems. Since there

is no reason – with the exception of the overbeaming effect discussed above – why radiation exposure as described by the dosimetric parameters DLP_{exam} and E_{exam} should be considerably higher at quad- than at dual-slice scanners, there is a considerable potential for dose reduction at quad-slice systems by optimising scan protocols and better education and training of medical and technical staff. As a first step in this direction, all owners of MSCT scanners who responded to our inquiry were informed in a feedback action about the dosimetric quantities that were estimated for the standard examinations based on their indications in the questionnaire in relation to the mean values established in the German SSCT survey in 1999. If an MSCT owner already participated in the former survey, a direct comparison of the scan parameters and dose values between his new MSCT and his old SSCT scanner was also provided.

Conclusion

The increase in the average dose per CT examination determined in the present study for quad-slice systems with respect to SSCT is not as alarming as it might have appeared from recent studies (e.g. [22]) in which heavily optimised SSCT protocols were compared to MSCT exposure settings at the begin of their optimisation process. Another trend, however, gives cause for concern, namely the large rise in the annual number of CT procedures carried out per MSCT scanner. According to the informa-

tion provided in the questionnaires, this number has significantly increased by 63% at quad-slice compared with single-slice systems. Although there may be a bias in the quad-slice data due to the fact that expensive MSCT scanners are presently mainly only afforded by institutions with a high workload, it can be assumed that the improved clinical efficacy and new applications will nevertheless lead to rising examination frequencies. If this rise is not compensated by an equivalent reduction of the total number of patients investigated at SSCT systems, which cannot be decided on the basis of the available data, it will result in a substantial increase in the collective effective dose arising from CT procedures. This trend may be justified in part by an increased benefit for the patient, as, for example, by performing coronary angiography by MSCT scanning instead of by an interventional X-ray procedure. For these dedicated applications, scientific evidence has to be warranted by sound clinical studies. In general, however, the danger of an uncontrolled increase of patient exposure due to CT procedures has to be limited by a clear medical justification in each individual case, independent of whether a standard examination is carried out or a new MSCT application such as coronary angiography, coronary calcium scoring or virtual colonoscopy.

Acknowledgements The authors thank all respondents to our survey for their support and the staff of the eight CT facilities where phantom measurements were performed for their excellent collaboration. Furthermore, the technical support of R. Truckenbrodt (BfS, Munich, Germany) is gratefully acknowledged.

References

- Kalender WA, Seissler W, Klotz E, Vock O (1990) Spiral volumetric CT with single-breath-hold technique, continuous transport, and scanner rotation. *Radiology* 176:181–183
- Liang Y, Kruger RA (1996) Dual-slice spiral versus single-slice spiral scanning: comparison of the physical performance of two computed tomography scanners. *Med Phys* 23:205–220
- Klingenbeck-Regn K, Schaller S, Flohr T, Ohnesorge B, Kopp AF, Baum U (1999) Subsecond multi-slice computed tomography: basics and applications. *Eur J Radiol* 31:110–124
- Fuchs TO, Kachelriess M, Kalender WA (2000) System performance of multislice spiral computed tomography. *IEEE Eng Med Biol Mag* 19:63–70
- Fuchs T, Kachelriess M, Kalender WA (2000) Technical advances in multi-slice spiral CT. *Eur J Radiol* 36:69–73
- Rubin GD (2000) Data explosion: the challenge of multidetector-row CT. *Eur J Radiol* 36:74–80
- Dawson P, Lees WR (2001) Multi-slice technology in computed tomography. *Clin Radiol* 56:302–309
- Rydberg J, Buckalter KA, Caldemeyer KS, Phillips MD, Conces DJ, Aisen AM, Persohn SA, Kopecky KK (2000) Multisection CT: scanning techniques and clinical applications. *Radiographics* 20:1787–1806
- Berland LL, Smith JK (1998) Multidetector-array CT: once again, technology creates new opportunities. *Radiology* 209:327–329
- Kopecky KK, Buckwalter KA, Sokiranski R (1999) Multi-slice CT: spirals past single-slice CT in diagnostic efficacy. *Diagn Imaging* 21:36–42
- Knez A, Becker CR, Leber A, Ohnesorge B, Becker A, White C, Haberl R, Reiser MF, Steinbeck G (2001) Usefulness of multislice spiral computed tomography angiography for determination of coronary artery stenoses. *Am J Cardiol* 88:1191–1194
- Nieman K, Rensing BJ, van Geuns RJ, Munne A, Ligthart JM, Pattynama PM, Krestin GP, Serruys PW, de Feyter PJ (2002) Usefulness of multislice computed tomography for detecting obstructive coronary artery disease. *Am J Cardiol* 89:913–918
- Schroeder S, Kopp AF, Ohnesorge B, Loke-Gie H, Kuettner A, Baumbach A, Herdeg C, Claussen CD, Karsch KR (2002) Virtual coronary angiography using multislice computed tomography. *Heart* 87:205–209
- Gerber TC, Kuzo RS, Karstaedt N, Lane GE, Morin RL, Sheedy PF, Safford RE, Blackshear JL, Pietan JH (2002) Current results and new developments of coronary angiography with use of contrast-enhanced computed tomography of the heart. *Mayo Clin Proc* 77:55–71

15. Hong C, Becker CR, Schoepf UJ, Ohnesorge B, Bruening R, Reiser MF (2002) Coronary artery calcium: absolute quantification in nonenhanced and contrast-enhanced multi-detector row CT studies. *Radiology* 223:474–480
16. Bruzzi JF, Moss AC, Fenlon HM (2001) Clinical results of virtual colonoscopy. *Eur Radiol* 11:2188–2194
17. Luboldt W, Fletcher JG, Vogl TJ (2002) Colonography: current status, research directions and challenges. Update 2002. *Eur Radiol* 12:502–524
18. UNSCEAR (2000) 2000 report, vol I. Sources and effects of ionizing radiation. Annex D: Medical radiation exposures. United Nations Sales Publications
19. Bundesamt für Strahlenschutz. Jahresbericht 2000. <http://www.bfs.de>
20. European Commission (1999) Report EUR 16262 EN: European guidelines on quality criteria for computed tomography
21. Seifert H, Hagen T, Bartylla K, Blass G, Piepgras Ü (1997) Patient doses from standard and spiral CT of the head using a fast twin-beam system. *Br J Radiol* 70:1139–1145
22. Giacomuzzi SM, Torbica P, Rieger M, Lottersberger C, Peer S, Peer R, Perkmann R, Buchberger W, Bale R, Mallouhi A, Jaschke W (2001) Evaluation of radiation exposure with single-slice and a multi-slice CT system (a phantom study). *Fortschr Röntgenstr* 173:643–649
23. Moro L, Bolsi A, Baldi M, Bertoli G, Fantinato D (2001) Single-slice and multi-slice computerized tomography: dosimetric comparison with diagnostic reference levels. *Radiol Med* 102:262–265
24. Galanski M, Nagel HD, Stamm G (2001) CT-Expositionspraxis in der Bundesrepublik Deutschland. *Fortschr Röntgenstr* 173:R1–R66
25. Nagel HD, Galanski M, Hidajat N, Maier W, Schmidt T (2000) Radiation exposure in computed tomography: fundamentals, influencing parameters, dose assessment, optimisation, scanner data, terminology. COCIR, Frankfurt
26. Stamm G, Nagel HD (2002) CT-Expo: ein neuartiges Programm zur Dosis-evaluierung in der CT. *Fortschr Röntgenstr* 174:1570–1576
27. ICRP Publication 60 (1991) 1990 Recommendations of the International Commission on Radiological Protection. Ann ICRP 21/1–3. Elsevier, Oxford
28. Zankl M, Panzer W, Drexler G (1991) The calculation of dose from external photon exposures using reference human phantoms and Monte Carlo methods. Part IV. Organ doses from tomographic examinations. GSF report 30/91, Neuherberg
29. Kramer R, Zankl M, Williams G, Drexler G (1982) The calculation of dose from external photon exposures using reference human phantoms and Monte Carlo methods. Part I. The male (Adam) and female (Eva) adult mathematical phantoms. GSF report S-885, Neuherberg
30. Shrimpton PC, Jones DG, Hillier MC, Wall BF, Leheron JC, Faulkner K (1991) Survey of CT practice in the UK. Part 2. Dosimetric aspects. NRPB-249, HMSO, 48, London
31. European Commission (2000) Report EUR 19604 EN: Recommendations for patient dosimetry in diagnostic radiology using TLD
32. Huda W, Sandison GA (1984) Estimation of mean organ doses in diagnostic radiology from Rando phantom measurements. *Health Phys* 47:463–467
33. Bushberg JT, Seibert JA, Leidholdt EM, Boone JM (2002) The essential physics of medical imaging, 2nd edn. Lippincott Williams and Wilkins, Philadelphia
34. Kopp AF, Heuschmid M, Claussen CD (2002) Multidetector helical CT of the liver for tumor detection and characterization. *Eur Radiol* 12:745–752